PERGAMON

International Journal of Solids and Structures 38 (2001) 5915–5934

INTERNATIONAL JOURNAL OF SOLIDS and STRUCTURES

www.elsevier.com/locate/ijsolstr

# Statistical modeling of heterogeneous micro-beams

Eli Altus *

*Faculty of Mechanical Engineering, Technion, Israel Institute of Technology, Haifa 32000, Israel*

Received 18 May 2000; in revised form 4 October 2000

**Abstract**

Statistical characteristics (averages and variances) of heterogeneous, small size beams (micro-beams), composed of micro-elements (grains) of randomly distributed stiffness (isotropic) is studied. Only longitudinal variations are considered. Element to beam size (length) ratio is not negligible and the use of an equivalent homogeneous structure with the classical effective material properties is not sufficient. Using standard statistical tools (probability density and correlation functions), it is shown that for indeterminate cases, even average deflections (obtained explicitly) are load dependent, and are *not* identical with their corresponding homogeneous case. Bounds for the statistical dispersion of deflections and reaction forces are found analytically for some cases of weak heterogeneity. It is shown that dispersion parameters for indeterminate problems can be obtained by superposition (using both averages and dispersion data) of corresponding determinate cases, leading to reciprocal type relations. 

*Keywords:* Beams; Elasticity; Probability; Heterogeneity; Micro-mechanics; Statistical dispersion

## 1. Introduction and motivation

The analysis, prediction and testing of the mechanical behavior (stiffness, strength, creep, fatigue, wear, etc.) of micro-electro mechanical systems (MEMS) and other "small scale" structures, pose new challenges in many fields: development of processing technologies, measurement tools, material analysis and characterization etc.

One of the emerging problems in the design of micro-mechanical systems, which is specifically related to their size, is the relatively small ratio between the characteristic size of micro-scale-structures (MSS), like beams, plates, etc., and the size of their basic elements (crystal grains). MSS having several microns (and less) thickness, made from polycrystals with grains of the same size order, are routinely built and used for many applications. For these working scales, the homogeneous assumption (using effective properties) may not be valid.

The common production method of MSS consists of preparing many "identical" parts from a single polycrystal (metal or ceramic) sheet (film, wafer). Since the local crystal direction and grain geometry vary from point to point, all MSS are effectively identical "in some average sense", when their characteristic size is sufficiently large compared to the size of a single grain. For small size (say, less then 20 grains in at least

* Tel.: +972-4-829-3157; fax: +972-4-832-4533.
*E-mail address:* merelal@tx.technion.ac.il (E. Altus).

0020-7683/01/$ - see front matter 
PII: S0020-7683(00)00385-1

one "active" direction), each MSS cut from the same wafer will produce a different deflection for the same external load (stiffness distribution), or might have a different strength (external load at breakage, yield etc.). When high performance and reliability is required, as for micro-size sensors, actuators etc, this distribution (reliability), *not* seen in macro-size structures, may be a crucial factor in their design, production and control. Standard "effective stiffness" methods (Hashin and Shtrikman, 1962; Willis, 1977; Kroner, 1986), which use a representative volume element (RVE), are not sufficient here, due to the finite size of the inhomogeneous material space.

A practical example of a basic MSS that will be studied here resembles a polysilicon simple cantilever beam, often used in MEMS (Howe and Muller, 1983; Howe, 1988; Madou, 1997; Jones et al., 1998) under various loads. Polysilicon is one of the prime materials used extensively in the MEMS and micro-electronic industry (Kamins, 1998). It is an ideal brittle (linear elastic) material at room temperature and there are verified methods for the production of wafers with controlled grain size (0.03–100 μm) and orientation (from preferred 110 to random) distributions (Kamins, 1998).

A few hundred micro-beams may be produced from a single polysilicon plate by MEMS technologies (Serre et al., 1998, 1999), from which the statistical data is derived. Recent experimental capabilities of examining the detailed material micro-structures is pushing the theoretical work on effective properties of materials to new levels of insight (Beran et al., 1996; Mason and Adams, 1999). These new findings show that crystallographic texture, especially various statistical correlation functions between elastic properties of neighbor grains, play a major role in the construction of overall effective properties.

In spite of the above progress, the problem of random mechanical response of micro-structures (deflections, forces etc.), emerging from the element/structure size ratio received very little attention, and has been noticed only recently (Madou, 1997). A preliminary study, which addresses a simple cantilever problem (Mirfendereski et al., 1992) used finite element analysis to show the general statistical dispersion effect, but the insight level is still in its infancy. Recent theoretical studies on "small RVEs", which also focus on the statistical distribution of small-scale composite structures are also related to the present study and are noted (Drugan and Willis, 1996; Ostoja-Starzewski, 1998). Of special relevance is the study of a heterogeneous beam (Beran, 1998), with special crystal anisotropy, for which the grain size is in the order of the thickness, but very small compared to the beam length. This case is not treated here.

Therefore, the relation between deflection statistics of micro-beams and material texture is the main goal of this study. Mechanical behavior (bounds on the average deflections) of heterogeneous beams were studied in the past (Somoroff, 1970), but no consideration has been given to the above "element to global" size effects, and no dispersion analysis presented.

The general heterogeneous beam problem has few complexities: non-isotropic elements (i.e., coupling between extension and shear), heterogeneity in three directions and non-linear effects (geometrical or material). This study assumes Bernoulli linear beams, the anisotropic crystal effect are neglected and the heterogeneity (variations) is considered in the longitudinal direction only. This study is a first approximation towards a more realistic micro-beams case, in which transverse (through the thickness and/or width) heterogeneity will also be taken into account.

The elementary problem of a heterogeneous cantilever beam under a concentrated load is studies first (Section 2), considering discrete and continuous stiffness distribution. A generalization to a single indeterminacy beam under general loading is studied in Section 3. Finally, multiply constraint case under general loading is analyzed in Section 4.

Kroner's (1986) elegant mathematical notations are followed here. Statistical properties of random functions (say, $S$) are: $\langle S\rangle \equiv$ ensemble average, $S' = S - \langle S\rangle \equiv$ deviation from the average, $\overline{S} = S/\langle S\rangle \equiv$ normalization by the average, $\widetilde{S} = S/S_0 \equiv$ normalization by another non-random value, $\overline{S}' = S'/\langle S\rangle \equiv$ normalized deviation. Therefore, $\langle(\overline{S}')^2\rangle$ is the normalized variance of $S$. Mathematical definitions and relations and some manipulations are outlined in the appendix. Other notations are directly presented in the text.

## 2. Simple cantilever beam under a concentrated load

### 2.1. Discretely varying compliance

Consider a simple "Bernoulli cantilever" of length $L$, loaded by a concentrated force $F$ at the free edge (shown schematically in Fig. 1).

The beam is made of $n$ elements (grains) of equal size, each having a Young modulus (compliance) $E_k(S_k)$ which is a random variable. Cross-section properties (relevant moment of inertia $I$) is equal for all elements. The aim is to find basic statistical parameters (average and variance) of the deflection at the edge $(w(x=0))$. Denote the internal bending moment by $M(x)$ and the total elastic energy by $U$, for each realization (linear analysis, small deformations), we have

$$w(x=0,n)=\frac{\partial U}{\partial F}=\frac{\partial}{\partial F}\int_0^L\frac{M^2}{2E(x)I}\mathrm{d}x=\frac{F}{I}\int_0^L\frac{x^2}{E(x)}\mathrm{d}x=\frac{F}{I}\left[\sum_{k=1}^{n}\int_{(k-1)L/n}^{kL/n}\frac{x^2}{E_k}\mathrm{d}x\right]$$
$$=\frac{FL^3}{3I}\sum_{k=1}^{n}\left(S_k\frac{k^3-(k-1)^3}{n^3}\right)=\frac{FL^3}{3I}\sum_{k=1}^{n}(S_kC_k), \tag{2.1}$$

where

$$S_k=E_k^{-1},\qquad C_k=\frac{k^3-(k-1)^3}{n^3}. \tag{2.2}$$

$C_k$ is the "relative deflection weight" of element $k$, which is parabolic with the distance from the edge $(kL/n)$. It means that the sensitivity of $w(0)$ to a stiffness (compliance) variation is higher for elements near the fixed end $(x=L)$. Notice also that since Eq. (2.1) is valid for a uniform (homogeneous) beam too, and $C_k$ is independent of $S_k$,

$$\sum_{k=1}^{n}(C_k)=1. \tag{2.3}$$

Taking $N$ samples from the same plate ($N$ large enough), we get

$$\langle w(0,n)\rangle=\frac{1}{N}\sum_{K=1}^{N}\frac{FL^3}{3I}\sum_{k=1}^{n}(S_kC_k)=\frac{FL^3}{3I}\sum_{k=1}^{n}(\langle S_k\rangle C_k). \tag{2.4}$$

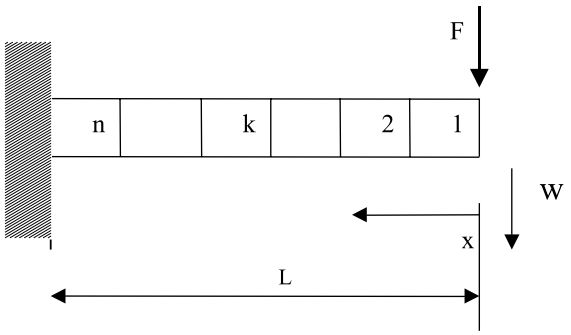


Fig. 1. Multigrain beam. Each grain takes the full thickness.

Suppose that all compliances $S_k$ are random variables of the same statistical distribution (statistical homogeneity), having an average value

$$\langle S_k \rangle = \langle S \rangle. \tag{2.5}$$

Then,

$$\langle w(0;n) \rangle = \frac{FL^3}{3I} \langle S \rangle = w_{(\mathrm{h})}, \tag{2.6}$$

where $w_{(\mathrm{h})}$ is the end deflection of an equivalent homogeneous beam having a compliance $\langle S \rangle$. Therefore, Eq. (2.6) coincides with the classical "effective moduli solution" using an RVE. The above is valid for *any* spatial (statistically homogeneous) compliance distribution $S_k$. When $S_k$ and $S_m$ are uncorrelated $(m \neq k)$, $w(0;n)$ is a sum of uncorrelated random functions, multiplied by non-random factors $C_k$ (2.2). Therefore, by the central mean theorem, the probability of $w(0;n)$ converges to a normal distribution as $n \to \infty$ with a constant average of value as in Eq. (2.6). The deflection variance is found by

$$\langle \overline{w}'^2 \rangle = \frac{\langle w'^2 \rangle}{\langle w_{(\mathrm{h})}^2 \rangle} = \left\langle \left( \sum_{k=1}^{n} C_k (\overline{S}_k - 1) \right)^2 \right\rangle = \left\langle \left( \sum_{k=1}^{n} C_k \overline{S}'_k \right)^2 \right\rangle = V_0 + \Delta V_0, \tag{2.7a}$$

$$V_0 = \left\langle \sum_{k=1}^{n} C_k^2 \overline{S}_k'^2 \right\rangle; \qquad \Delta V_0 = 2 \left\langle \sum_{m=1}^{n} \left( \sum_{k=m+1}^{n} C_k C_m \overline{S}'_k \overline{S}'_m \right) \right\rangle, \tag{2.7b}$$

where $V_0$ is the deflection variance of the non-correlated case and $\Delta V_0$ is the deviation due to such correlation. Then,

$$V_0 = \left( \sum_{k=1}^{n} C_k^2 \right) \langle \overline{S}_k'^2 \rangle = \left( \sum_{k=1}^{n} C_k^2 \right) V(\overline{S}). \tag{2.8}$$

It can be also shown that

$$\sum_{k=1}^{n} C_k^2 = \frac{1}{n^6} \left[ \frac{31}{5} (n+1) - 15(n+1)^2 + 17(n+1)^3 - 9(n+1)^4 + \frac{9}{5} (n+1)^5 - 1 \right]. \tag{2.9}$$

Therefore, for the uncorrelated case, the variances of $S$ and $w(0)$ for large $n$ are related by:

$$V_0(\overline{w}(0; n \gg 1)) \cong \frac{9}{5n} V(S). \tag{2.10}$$

It is useful to compare this result with the 'equal weight' case. There, $C_k = 1/n$ and the factor in Eq. (2.10) is simply $1/n$. Therefore, the value (9/5) reflects the increased statistical dispersion of the end deflection due to an unequal contribution of the grains as a function of their position. It will be shown that the equal weight case gives a lower dispersion bound.

For demonstration purposes, consider a realistic example of a polysilicon beam made from 15 grains (order of magnitude). The modulus of each element is a function of the crystal orientation. For silicon, the maximum and the minimum Young's modulus values are 190 and 130 GPa respectively (Wortman and Evans, 1965). Using Eq. (2.10) and an equal distribution of modulus in the above range we get

$$V(\overline{S}) \cong 0.13^2 \quad \Rightarrow \quad V(\overline{w}(0; n = 15)) \cong 0.045^2. \tag{2.11}$$

Finite element calculations of a cantilever beam using Monte–Carlo simulations have been done elsewhere (Mirfendereski et al., 1992). There, the anisotropic effects of polysilicon were taken into account, with no neighbor correlation. The morphology consisted of $n \sim 15$ elements along the beam length and an average of less than two grains through the thickness. It was found that $V(\overline{w}(0; n = 15)) \cong 0.04^2$, which is in

a good agreement with Eq. (2.11). However, as will be seen in the following, real specimens are expected to show much higher dispersion values. The reason is that neighbor crystal orientations are definitely correlated. Therefore, Eq. (2.11) can be considered as a lower estimate for a real micro-beam.

The most important factor of the statistically correlated case is the ratio $\Delta V_0/V_0$, which reflects the relative two points' correlation effect. From Eq. (2.7b), the translation symmetry can be used. Define the two-point correlation function by

$$\phi_j = \langle \overline{S}'_k \overline{S}'_{k+j} \rangle, \quad 0 < \phi_j < 1. \tag{2.12}$$

Then,

$$\Delta V_0 = 2\sum_{j=1}^{n-1}\sum_{k=1}^{n-j} C_k C_{k+j} \langle \overline{S}'_k \overline{S}'_{k+j} \rangle = 2\sum_{j=1}^{n-1} \phi_j \sum_{k=1}^{n-j} C_k C_{k+j} = 2\sum_{j=1}^{n-1} \phi_j \Phi_j, \tag{2.13}$$

where $\Phi_j$ can be written as:

$$\Phi_j = \frac{1}{10n^6}\left[2n - 2j + 15n^2 j + 30j^2 n^3 - 45jn^4 - 10n^3 - 5j^3 - 3j^5 + 18n^5\right] \tag{2.14}$$

with a leading term of $9/5$ too. Eq. (2.13) is a sum of two point correlation terms which vanish as $j$ (the distance between neighbors) becomes large, and the real distribution function will have to be taken from experiments. However, important insight can be achieved even if a simple function is assumed. Consider the first-order auto-regression model (Box and Jenkins, 1970):

$$\phi_j = \phi^j, \tag{2.15}$$

where $\phi_1 = \phi$ is the only coefficient controlling the two points correlation. $\phi = 0$ means that there is no correlation between the compliance of any two grains, while $\phi = 1$ represents a perfect correlation, i.e., all grains of the same beam have the same compliance (essentially, beams of a single grain). Between these extremes, $\phi$ is directly related to the correlation "length" by the following:

$$\phi_j = \phi^j = \exp\left[j \ln(\phi)\right] = \exp\left[-j/j_{\mathrm{ch}}\right], \tag{2.16}$$

where $j_{\mathrm{ch}}$ is the characteristic correlation distance

$$j_{\mathrm{ch}} = -1/\ln(\phi). \tag{2.17}$$

In real polycrystals, $j_{\mathrm{ch}}$ is in the order of the average grain size. Having $\phi$, it is possible to plot $\Delta V_0/V_0$ vs $j_{\mathrm{ch}}$ for various values of $n$ and examine the correlation effect, as shown in Fig. 2. Results for five values of $n$ over three orders of magnitude show that the curve converges to a linear relation as $n > 2000$. In all cases shown, the correlation effect on the deflection variance is considerable. For example, for $n = 60$ and an effective correlation distance of only 2, the relative deviation $\Delta V_0/V_0$ is $\sim$2.6, i.e., about 60% increase in the deflection statistical standard deviation as compared to the uncorrelated case.

The asymptotic line in Fig. 2 can be found analytically and permits important insight. $j_{\mathrm{ch}}$ can be considered roughly as a distance beyond which no correlation exists. Therefore, it is expected that the edge deflection variance should be the same as for a beam having $n/2j_{\mathrm{ch}}$ non-correlated grains (this is since the correlation range extends to both sides of each grain). It means that

$$\frac{\Delta V_0}{V_0} = \frac{V_{\mathrm{u}}[n_{\mathrm{u}} = n/2j_{\mathrm{ch}}] - V_{\mathrm{u}}[n_{\mathrm{u}} = n]}{V_{\mathrm{u}}[n_{\mathrm{u}} = n]}, \tag{2.18}$$

where $V_{\mathrm{u}}$ is the variance for the uncorrelated case with $n_{\mathrm{u}}$ elements. Since $V_{\mathrm{u}}$ is proportional to $1/n_{\mathrm{u}}$ (2.9), we get from Eq. (2.18)

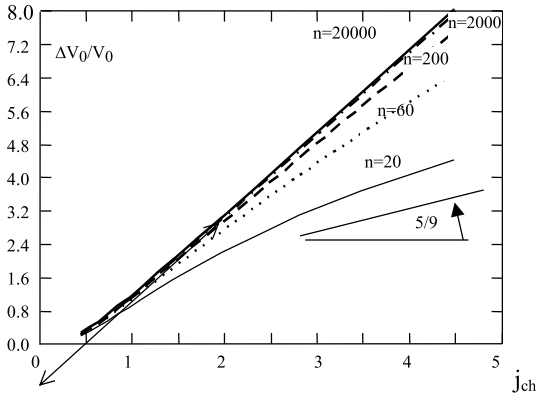


Fig. 2. Effect of correlation distance ($j_{ch}$) on the relative dispersion of cantilever beam end deflection.

$$\frac{\Delta V_0}{V_0}(n \to \infty) = \frac{2j_{ch}/n - 1/n}{1/n} = 2j_{ch} - 1 \tag{2.19}$$

which means that the asymptotic curve of Fig. 2 should be linear with a slope of 2, and cut the $j_{ch}$ line at 0.5. The asymptotic relation of Eq. (2.19) was added to Fig. 2 (arrows on edges) for comparison, and confirms the above predictions. Note that the results for $j_{ch} < 0.5$ (i.e., a "bundle" below 1 grain) is not physical.

Another asymptotic behavior is seen if $j_{ch}$ approaches $n$ ($\phi \to 1$). The beam acts like a single grain, and therefore, from Eqs. (2.7a) and (2.7b)

$$\frac{\Delta V_0}{V_0}(j_{ch} \to n) = \frac{5n}{9} - 1 \tag{2.20}$$

which can be confirmed by checking that the asymptotic slopes in Fig. 2 for large $j_{ch}$ tend to 5/9. It can be seen that the $n = 20$ line approaches this value "quicker" than the other lines, since $j_{ch}$ approaches $n$ "faster" for smaller $n$.

### 2.2. Continuously varying compliance

The aim of this paragraph is to compare the previous analysis to the case where $S(x)$ is a continuously varying function, and see if new insight is gained. Assume the same cantilever, loaded by a concentrated force $F$ at $x = 0$. From Eq. (2.1), for a statistically homogeneous beam

$$\langle w(0)\rangle = \frac{F}{I}\int_0^L x^2\langle S(x)\rangle\,\mathrm{d}x = \frac{F}{I}\langle S(x)\rangle\int_0^L x^2\,\mathrm{d}x = \frac{FL^3}{3I}\langle S\rangle = w_{(h)} \tag{2.21}$$

as expected. Using Eqs. (2.1) and (2.21), the displacement variance is found by

$$V(\overline{w}(0)) = \int_0^1\int_0^1 x_1^2x_2^2\langle\overline{S}_1'\overline{S}_2'\rangle\,\mathrm{d}x_1\,\mathrm{d}x_2 \tag{2.22}$$

where from here on, all position values ($x$) are normalized by $L$, and

$$\overline{S}'(x_k) \equiv \overline{S}_k' = \overline{S}(x_k) - 1. \tag{2.23}$$

Similar to the characteristic length ($j_{ch}$) considerations for the discrete distribution, consider an idealized case where there is a complete compliance correlation inside a specific range $\Delta x/L = \lambda$, and a totally non-

correlated relation outside this range. A good (but not fully identical) example is the case where neighbor grain orientation is uncorrelated, but fully correlated within the grain. Then,

$$\langle \overline{S}_1' \overline{S}_2' \rangle = \left\{ \begin{array}{ll} \langle \overline{S}'^2 \rangle; & \left| \frac{x_2 - x_1}{L} \right| < \lambda \\ 0; & \text{otherwise} \end{array} \right\}, \quad \lambda \ll 1. \tag{2.24}$$

Inserting Eq. (2.24) in Eq. (2.22) we have

$$V(\overline{w}(0)) = \frac{F^2}{I^2} \int_0^1 \langle \overline{S}'^2 \rangle x_1^2 \, \mathrm{d}x_1 \int_{x_1-\lambda}^{x_1+\lambda} x_2^2 \, \mathrm{d}x_2 = \frac{F^2 L^6}{I^2} \langle \overline{S}'^2 \rangle \left( \frac{1}{5} 2\lambda + \frac{1}{9} 2\lambda^3 \right). \tag{2.25}$$

For small enough, but still finite $\lambda$ (equivalent to large $n$ in the discrete heterogeneous case), the displacement and compliance variances are related by

$$V(\overline{w}(0)) = V(\overline{S}) \eta_2^2 2\lambda, \quad \eta_2 = \left(\tfrac{9}{5}\right)^{1/2}, \tag{2.26}$$

where $\eta_2$ is the second-order "dispersion factor". It can be shown that $\eta_2$ is invariant with regard to the specific "shape" of $\langle S_1' S_2' \rangle$ inside $\lambda$, but on the average value only. Thus, $\lambda$ is a convenient scale parameter for defining three distinct levels of morphology, each deserving a different degree of analysis: (a) macroscale ($\lambda \to 0$), for which the classical RVE approach is appropriate, (b) mesoscale ($\lambda \ll 1$), for which only the correlation length is important, and (c) micro-scale ($\lambda \sim 1$), where the full correlation function is needed. The mesoscale receives the highest attention in the sequal, due to the relative ease of analytical manipulations and the easy insight. An additional intermediate range ($\lambda \sim 0.1$), where second-order perturbations is needed, are also important, but will not be studied here.

Returning to Eq. (2.26), the value of $\eta_2$ comes directly from the *power* (2 in this case) of $x$ in the basic beam deflection equation (2.1): $9 = (2+1)(2+1)$, $5 = (2 \times 2) + 1$. This power is related to the square of the bending moment $M(x)$.

In order to generalize this observation, assume that the bending moment is some power function of $x$. It is easy to show that

$$M(x) \propto x^k \to \eta = \frac{(2k+1)^2}{(2k)^2 + 1} = 1 + \frac{4k}{4k^2 + 1} \tag{2.27}$$

from which $\eta_2$ and $k$ are related by

$$-\infty < k < \infty \leftrightarrow 0 < \eta_2 < 2^{1/2}, \tag{2.28}$$

so that $\eta_2$ is bounded. The loading function for these bounds can be also found. If $q(x_1)$ is the distributed external loading function, then

$$M(x) = \int_0^x x_1 q(x_1) \, \mathrm{d}x_1. \tag{2.29}$$

Then,

$$\eta_2^+ = \eta_2(k = 1/2) \to q(x, \eta_2^+) \propto x^{-(3/2)}, \tag{2.30}$$

$$\eta_2^- = \eta_2(k = -1/2) \to q(x, \eta_2^-) \propto x^{-(5/2)}, \tag{2.31}$$

where $\eta_2^+$, $\eta_2^-$ are upper and lower bounds. However, from the finiteness of the elastic energy density we have also the condition $k > 0$. Therefore, part of the domain in Eq. (2.31) is not physical and Eqs. (2.28), (2.30) and (2.31) are modified to be

$$0 < k < \infty \leftrightarrow 1 < \eta_2 < 2^{1/2}, \qquad k(\eta_2^-) = 0 \text{ or } \infty, \qquad k(\eta_2^+) = 1/2. \tag{2.32}$$

Relations (2.32) are of major importance. They give *bounds* on the displacement statistical dispersion of a heterogeneous beam *for load dependent cases*. More specifically, the minimum dispersion is either when the internal bending moment is "evenly spread" (as in the case of a pure external moment at $x = 0$) or when the load is "extremely" concentrated near the clamped edge ($x = L$). The first is the equal statistical weight case and the second is the case where only the $S(x \sim 1)$ value is important. On the other limit, maximum dispersion occurs when $q(x)$ is proportional to $x^{-3/2}$.

Consider next the third-order normalized dispersion function $\eta_3$ of $w(0)$

$$d_3(w(0)) = \left( \frac{\langle (w'(0))^3 \rangle}{\langle w(0) \rangle^3} \right)^{1/3} \tag{2.33}$$

and follow the same conditions as in Eq. (2.24)

$$\langle \overline{S}'_1 \overline{S}'_2 \overline{S}'_3 \rangle = \left\{ \begin{array}{ll} \langle \overline{S}'^3 \rangle; & |x_2 - x_1| \leqslant \lambda \text{ and } |x_3 - x_2| \leqslant \lambda \\ 0; & \text{otherwise} \end{array} \right\}, \tag{2.34}$$

the third-order relation, equivalent to Eq. (2.26) is then found as

$$d_3(w(0)) = d_3(\overline{S})(\eta_3)^3 \lambda^{2/3}, \quad \eta_3^3 = \tfrac{27}{7}. \tag{2.35}$$

Analyzing the case of a power function for the internal moment, as in Eq. (2.27), we get

$$M(x) \propto x^k \to \eta_3^3 = \frac{(3k+1)^3}{(3k)^3 + 1} \tag{2.36}$$

for which,

$$0 < k < \infty \leftrightarrow 1 < \eta_3^+ < 4^{1/3}, \quad k(\eta_3^-) = 0 \text{ or } \infty, \quad k(\eta_3^+) = 1/3 \tag{2.37}$$

and the external loading for the maximum dispersion is

$$q(x, \eta_3^+) \propto x^{-(5/3)}. \tag{2.38}$$

This procedure can be done for any dispersion power $p$, which yields a set of upper bounds

$$1 < \eta_p^+ < 2^{1-1/p}, \quad q(\eta_p^+) \propto x^{2^{p-1}-2}. \tag{2.39}$$

Note that each upper bound is associated with a different external loading function, but lower bounds are always related to the case of a concentrated external moment (homogeneous loading). Also,

$$p \gg 1 \to \eta_p \approx 2, \quad q \propto x^{-2} \tag{2.40}$$

and from Eq. (2.39), a general range between the two bounds is finally received for the whole statistical spectrum and a general loading function

$$2^{1/2} < \eta^+ < 2, \quad \eta^- = 1. \tag{2.41}$$

## 3. Heterogeneous beam – indeterminacy of one degree

### 3.1. Field equations

Consider a cantilever beam clamped on one side and simply supported on the other, as seen in Fig. 3. The beam is loaded externally by a distributed force $q(x_1)$, which is *not* random.

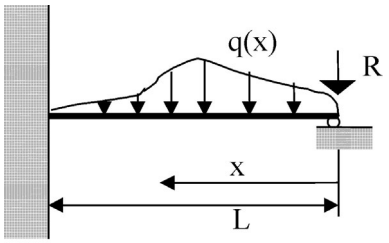


Fig. 3. A non-determinate (1°) Bernoulli beam.

We are interested in finding statistical parameters of the displacement $w$ at any point $x$. It is clear that, compared to the previous (determinate) case, $w(x)$ cannot be found by direct integration, and the governing equation for the force $R$ will have to be implemented in the solution. In fact, this is a simple version of a "mixed boundary condition" in elasticity. The bending moment is

$$M(x) = Rx + \int_{x_1=0}^{x} q(x_1)x_1\,\mathrm{d}x_1 + P(x_1 - x)H(x_1 - x), \tag{3.1}$$

where $H$ is the common unit step function: (0 for $x_1 < x$ and 1 for $x_1 > x$). Calculation of $w(x)$ can be done by using the dummy force $P$ at $x$, and applying the minimum energy principle such that

$$w(x) = \left.\frac{\partial U}{\partial P}\right|_{P=0} = \int_{x_1=0}^{L} S(x_1)M(x_1)\left.\frac{\partial M}{\partial P}\,\mathrm{d}x_1\right|_{P=0}; \quad S(x) = [E(x)I]^{-1}. \tag{3.2}$$

Substituting Eq. (3.1) in Eq. (3.2) yields

$$w(x) = \int_{x_1=x}^{L} S(x_1)(x_1 - x)(Rx_1 + Q(x_1))\,\mathrm{d}x_1, \tag{3.3}$$

where $Q$ is the first moment of the distributed load

$$Q(x_1) = \int_{x_2=0}^{x_1} q(x_2)x_2\,\mathrm{d}x_2. \tag{3.4}$$

For later convenience, $Q$ is normalized by an arbitrary (non-random, to be defined) force $R_\mathrm{h}$ and Eq. (3.3) is written in the form

$$w(x) = \int_{x_1=x}^{L} [f(x,x_1)R_\mathrm{h}S(x_1) + g(x,x_1)RS(x_1)]\,\mathrm{d}x_1, \tag{3.5}$$

where $f$ and $g$ are:

$$f(x,x_1) = (x_1 - x)\widetilde{Q}(x_1); \qquad g(x,x_1) = (x_1 - x)x_1; \qquad \widetilde{Q} = Q/R_\mathrm{h}. \tag{3.6}$$

The form in Eq. (3.5) is identical to all beam problems having "one degree" indeterminancy. Therefore, the specific example in Fig. 3 is served for illustrative purposes only. Then, using the notation from Eqs. (A.1)–(A.5), Eq. (3.5) is written as

$$w(x) = L^3R_\mathrm{h}(f * S + \widetilde{R}g * S); \quad \widetilde{R} = R/R_\mathrm{h}, \tag{3.7}$$

where all distances ($x$) are normalized to $L$. Consider an equivalent *homogeneous* beam, with a uniform compliance equal to the effective one ($\langle S\rangle$ for Bernoulli beams). Then, $R_h$ is the reaction force associated with this beam, and is found from:

$$w_h(x=0) = L^3(f * \langle S\rangle + g * \langle S\rangle) = 0. \tag{3.8}$$

In the following, $R_h$ will be the solution of Eq. (3.8), so that $f$ and $g$ are related by (see Appendix A):

$$f * I + g * I = 0. \tag{3.9}$$

### 3.2. Calculation of $\langle R\rangle$

Our first interest is to find $\langle R\rangle$ and see if $\langle R\rangle = R_h$. For every heterogeneous beam from the ensemble, the deflection at $x = 0$ vanishes. Using Eq. (3.7) and averaging we have

$$\langle \widetilde{R}\rangle = -\langle (f * S)(g * S)^{-1}\rangle. \tag{3.10}$$

Note that $\widetilde{R}$ is not a function of $\langle S\rangle$. The non-linearity of Eq. (3.10) calls for approximation appropriate for "weak heterogeneity", i.e.,

$$|\overline{S}'| \ll 1; \quad \overline{S}' = (S - \langle S\rangle)\langle S\rangle^{-1}. \tag{3.11}$$

Then (see Appendix A):

$$\widetilde{R} = -(f * I + f * \overline{S}')(g * I + g * \overline{S}')^{-1} = \widetilde{R}|_{\overline{S}'=0} + \left.\frac{\delta \widetilde{R}}{\delta \overline{S}'}\right|_0 * \overline{S}' + \frac{1}{2}\left.\frac{\delta^2 \widetilde{R}}{\delta \overline{S}'^2}\right|_0 * * \overline{S}'\overline{S}' + \cdots \tag{3.12}$$

$f$ is a function of $\langle S\rangle$ (through $R_h$) and *not* $S'$, and can be taken as constant in Eq. (3.12). Then, using Eqs. (3.9), (3.10), and (3.12), and averaging, the first term in Eq. (3.12) equals to 1 (macro-scale contribution), and the second term vanishes. After few steps of algebra

$$\langle \widetilde{R}\rangle \cong 1 + (g * I)^{-2}(g * \langle \overline{S}'\overline{S}'\rangle * f^{\mathrm{T}}) - (g * I)^{-3}(f * I)(g * \langle \overline{S}'\overline{S}'\rangle * g^{\mathrm{T}}), \tag{3.13}$$

where Eq. (A.1):

$$\overline{S}'\overline{S}' \equiv \overline{S}'(x_1)\overline{S}'(x_2). \tag{3.14}$$

Eq. (3.13) proves that the average reaction force and the one based on a homogeneous beam with effective moduli are *not* the same. The normalized difference between the two (notice the expression symmetry) is

$$\overline{\Delta R_h} = \langle \widetilde{R}\rangle - R_h \cong \frac{g * \langle \overline{S}'\overline{S}'\rangle * g^{\mathrm{T}}}{g * II * g^{\mathrm{T}}} - \frac{g * \langle \overline{S}'\overline{S}'\rangle * f^{\mathrm{T}}}{g * II * f^{\mathrm{T}}} = \frac{g * \langle \overline{S}'\overline{S}'\rangle * (g+f)^{\mathrm{T}}}{g * II * g^{\mathrm{T}}}, \tag{3.15}$$

where Eqs. (A.10) and (3.9) have been used. By Eq. (A.7), Eq. (3.14) can be written in a symmetric form as

$$\overline{\Delta R_h} = \frac{1}{2}\,\frac{(f+g) * \langle \overline{S}'\overline{S}'\rangle * (f+g)^{\mathrm{T}} + g * \langle \overline{S}'\overline{S}'\rangle * g^{\mathrm{T}} - f * \langle \overline{S}'\overline{S}'\rangle * f^{\mathrm{T}}}{g * II * g^{\mathrm{T}}}. \tag{3.16}$$

Each of the symmetric terms in Eq. (3.16) is the variance of the end deflection of a *determinate* beam discussed in Section 2. Therefore, Eq. (3.16) expresses a type of superposition, which will be further explored later.

Of special interest are the specific functions $\langle \overline{S}'\overline{S}'\rangle$ (material) and $f$ (external loading), for which $\overline{\Delta R_h}$ is extremal. When mesoscale morphology range is considered, Eq. (3.15) reduces to

$$\overline{\Delta R_{\mathrm{h}}} = \lambda \langle \overline{S}'^2 \rangle \frac{g * (g+f)^{\mathrm{T}}}{g * II * g^{\mathrm{T}}}, \quad \lambda \ll 1. \tag{3.17}$$

Then, a linear relation between $\overline{S}'^2$ and $\overline{\Delta R_{\mathrm{h}}}$ is observed. As for the loading effect, assume a power function, as in Section 2, so that:

$$\widetilde{Q}(x) = x^k \Rightarrow g * f^{\mathrm{T}} = -\frac{(k+2)}{3(k+4)} \Rightarrow R_{\mathrm{h}} = -\frac{3}{k+2} \tag{3.18}$$

for which Eq. (3.17) is

$$\overline{\Delta R_{\mathrm{h}}} = \lambda \langle \overline{S}'^2 \rangle \left[ \frac{9}{5} - \frac{3(k+2)}{k+4} \right]. \tag{3.19}$$

Differentiating Eq. (3.19) with respect to $k$, equating to zero and taking into account the finiteness condition of the elastic energy density, we finally get

$$-1.2 < \frac{\overline{\Delta R_{\mathrm{h}}}}{\lambda \langle \overline{S}'^2 \rangle} < 0.3, \tag{3.20}$$

where the lower and upper bounds correspond to $k \to \infty$ and $k = 0$, respectively. The case for which $\overline{\Delta R_{\mathrm{h}}} = 0$ is also important:

$$k = 1 \Rightarrow q(x) = x^{-1} \Rightarrow f = -g \Rightarrow \Delta R_{\mathrm{h}} = 0. \tag{3.21}$$

Note that Eq. (3.21) corresponds to the case where the internal bending moment is zero, which is also a *determinate* case, for which $\overline{\Delta R_{\mathrm{h}}}$ is always zero (Section 2).

Another limit is the "infinite correlation range" case, i.e., beams of a single element (grain). For this case,

$$\overline{\Delta R_{\mathrm{h}}} = \overline{S}'^2 \frac{g * II * (g+f)^{\mathrm{T}}}{g * II * g^{\mathrm{T}}} = 0. \tag{3.22}$$

Combining Eq. (3.17) with Eq. (3.22), it is seen that $\overline{\Delta R_{\mathrm{h}}}$ has an extremum with regard to $\langle \overline{S}' \overline{S}' \rangle$ too, but it is not in the mesoscale range. Therefore, achieving analytic results is difficult.

### 3.3. Statistical variance of R

Using the same technique, it is now straightforward to calculate the variance of $R$, relative to $R_{\mathrm{h}}$

$$\langle (\widetilde{R})'^2 \rangle = \langle \widetilde{R}^2 \rangle - \langle \widetilde{R} \rangle^2 = \frac{V(R)}{R_{\mathrm{h}}^2}. \tag{3.23}$$

Using Eq. (3.13) and Eq. (A.33), and neglecting higher order terms, we have a relatively simple (and symmetric) result for the normalized variance:

$$\langle (\widetilde{R})'^2 \rangle = (\widetilde{R}_{,\overline{S}'})^2 \Big|_0 * * \langle \overline{S}' \overline{S}' \rangle = \frac{(f+g) * \langle \overline{S}' \overline{S}' \rangle * (f+g)^{\mathrm{T}}}{g * II * g^{\mathrm{T}}}. \tag{3.24}$$

Note that these symmetric forms are found when normalizing $R$ to the values of the equivalent homogeneous beam, and not to the real average value. For the latter we have

$$\langle (\overline{R})'^2 \rangle = \langle (\widetilde{R})'^2 \rangle \left[ 1 + 2g * \overline{S}' \overline{S}' * (g+f)^{\mathrm{T}} \right]. \tag{3.25}$$

The effect of external load on the statistical variance of $R$, is checked by inserting a power distribution for $\widetilde{Q}(x)$ and analyzing the sensitivity

$$\widetilde{Q}(x) = x^k \Rightarrow \langle (\widetilde{R})'^2 \rangle = \frac{9}{5} + \frac{(k+2)^2}{(2k+3)} - \frac{6(k+2)}{(k+4)}. \tag{3.26}$$

The only extremal point of Eq. (3.26), for which $k$ is real and positive (elastic energy density limitations) is

$$k = 1 \rightarrow f + g = 0 \rightarrow \langle (\widetilde{R})'^2 \rangle = 0 \tag{3.27}$$

which is the elementary lower bound, as in Eq. (3.20). The lack of an upper bound is not physical, but due to the apparent limits of the first order perturbation taken here.

To see the physical importance of Eq. (3.24), divide the beam problem into two parts: homogeneous, with compliance $\langle S \rangle$, and deviatoric, with compliance $S'$. For each part, there are two dual boundary conditions at $x = 0$. For the homogeneous part,

$$w(x=0) = 0 \rightarrow R = R_{\mathrm{h}} \quad \text{or} \quad R = R_{\mathrm{h}} \rightarrow w(x=0) = w_{\mathrm{h}}, \tag{3.28}$$

and for the heterogeneous (stochastic) part:

$$w(x=0) = 0 \rightarrow V(R) \quad \text{or} \quad R = R_{\mathrm{h}} \rightarrow V(w(x=0)). \tag{3.29}$$

Now, since

$$w_{\mathrm{h}}^2 = g * \langle S \rangle \langle S \rangle * g^{\mathrm{T}}; \qquad V(w(x=0)) = (f+g) * \langle S'S' \rangle * (f+g)^{\mathrm{T}}. \tag{3.30}$$

Eq. (3.24) can be written in a convenient form as

$$w_{\mathrm{h}}^2 V(R) = R_{\mathrm{h}}^2 V(w), \tag{3.31}$$

which is a *reciprocal relation*, similar to the familiar Maxwell theorem for linear structures. It may be used to find the variance of an indeterminate case, by the variance of the determinate one, and the homogeneous solution.

### 3.4. Displacement average

Using Eq. (3.7) and the displacement b.c., we have

$$w(x) = R_{\mathrm{h}} L^3 \langle S \rangle \left\{ f \underset{x}{\overset{1}{*}} \overline{S} - (f \underset{0}{\overset{1}{*}} \overline{S})(g \underset{0}{\overset{1}{*}} \overline{S})^{-1} (g \underset{x}{\overset{1}{*}} \overline{S}) \right\} \tag{3.32}$$

where integration limits are specified. As for $\langle R \rangle$, we consider the weak heterogeneity case (3.11) only. Expansion of Eq. (3.32) near $\langle S \rangle$, neglecting higher order terms and averaging we get,

$$\begin{aligned} \frac{\langle w(x) \rangle - w_{\mathrm{h}}(x)}{w_{\mathrm{h}}(x)} = \widetilde{\Delta} w_{\mathrm{h}}(x) &= \left[ \frac{g_x}{f_x + g_x} \right] \left\{ \widetilde{g} \underset{0}{\overset{1}{*}} ) - \widetilde{g} \underset{x}{\overset{1}{*}} ) \right\} \langle \overline{S}' \overline{S}' \rangle \left\{ ( \underset{0}{\overset{1}{*}} \widetilde{f}^{\mathrm{T}} - ( \underset{0}{\overset{1}{*}} \widetilde{g}^{\mathrm{T}} \right\} \\ &= \left[ \frac{g_x}{f_x + g_x} \right] \left[ \widetilde{\Delta} R_{\mathrm{h}} - \widetilde{g} \underset{x}{\overset{1}{*}} \langle \overline{S}' \overline{S}' \rangle \underset{0}{\overset{1}{*}} \left\{ \widetilde{f} - \widetilde{g} \right\}^{\mathrm{T}} \right] \end{aligned} \tag{3.33}$$

where $w_{\mathrm{h}}(x)$ is the displacement of a homogeneous beam with effective ($\langle S \rangle$) compliance and

$$\widetilde{g} \underset{0}{\overset{1}{*}} ) = g \underset{0}{\overset{1}{*}} )/g_0; \quad g_0 = g \underset{0}{\overset{1}{*}} I; \quad \widetilde{g} \underset{x}{\overset{1}{*}} ) = g \underset{x}{\overset{1}{*}} )/g_x; \quad g_x = g \underset{x}{\overset{1}{*}} I \quad \text{etc.} \tag{3.34}$$

For the mesoscale case, Eq. (3.29) is simpler:

$$\widetilde{\Delta} w_{\mathrm{h}}(x) = \left[\frac{g_x}{f_x + g_x}\right]\left[\widetilde{\Delta} R_{\mathrm{h}} - \lambda\langle \overline{S}'^2\rangle \frac{\overset{1}{x} * \{f+g\}^{\mathrm{T}}}{g_x g_0}\right]. \tag{3.35}$$

It is seen that for appropriate external load distributions and at some specific points on the beam, the displacement average can be equal to the "effective" solution (useful for design of micro-beams). Of course, in the special case mentioned above ($f = -g$), all average deviations vanish. However, in this case the deflection due to shear (not studied here) is dominant.

## 4. Multiply indeterminate heterogeneous beams

This section generalizes the analysis to the case of a beam with many constraints.

### 4.1. Field equations

Consider a beam loaded by external forces $q(x)$, and additional $n$ simply supported constraints at points $x_r$ $(1 < r < n)$. All dimensions, coordinates etc., are similar to the ones in Fig. 3. The bending moment in Eq. (3.1) is generalized to

$$M(x) = \sum_{r=1}^{N} R_r(x - x_r)H(x - x_r) + \int_{x_1=0}^{x} q(x_1)x_1\,\mathrm{d}x_1 + P(x_1 - x)H(x_1 - x). \tag{4.1}$$

Following the same steps as in Eqs. (3.2)–(3.4), we have

$$w(x) = \int_{x_1=0}^{1} [f_r(x, x_1)R_r^{(\mathrm{h})}S(x_1) + g_r(x, x_1)R_r S(x_1)]\,\mathrm{d}x_1, \tag{4.2}$$

where $f_r$ and $g_r$ are the components of two variable vectors

$$f_r(x, x_1) = \langle S\rangle L^3 H(x_1 - x)(x_1 - x)Q(x_1)(R_r^{(\mathrm{h})})^{-1}N^{-1}; \tag{4.3}$$

$$g_r(x, x_1) = \langle S\rangle L^3 (x_1 - x)(x_1 - x_r)H(x_1 - x)H(x_1 - x_r) \tag{4.4}$$

and the summation convention holds. $\mathbf{R}^{(\mathrm{h})}$ is the constraint force vector for an associated homogeneous beam having compliance $\langle S\rangle$. From Eq. (4.2), the $N$ displacement boundary conditions at $x = x_p$ $(1 \leqslant p \leqslant N)$ are

$$w_p = w(x = x_p) = f_{pr} * (I + \overline{S}')R_r^{(\mathrm{h})} + g_{pr} * (I + \overline{S}')R_r = 0; \tag{4.5}$$

$$f_{pr}(x_1) = f_r(x_p, x_1); \quad g_{pr}(x_1) = g_r(x_p, x_1), \tag{4.6}$$

where $\mathbf{f}$ and $\mathbf{g}$ are second-order tensor functions of one variable $(x_1)$. From Eq. (4.4), for the homogeneous beam, we get, similar to (3.9),

$$f_{rm} * I + g_{rm} * I = 0, \quad (\mathbf{f} + \mathbf{g}) * I = 0. \tag{4.7}$$

By definition,

$$\mathbf{G} = \mathbf{g} * I \tag{4.8}$$

is the symmetric, load independent Green's matrix for the homogeneous, determinate case, where only concentrated loads at $x_p$ exist, i.e., the displacement at one point due to a unit force at the other. Therefore, $\mathbf{g}$ *itself is a matrix density function*.

Eq. (4.5) in a vector form is

$$\mathbf{f} * (I + \overline{S}') \cdot \mathbf{R}^{(\mathrm{h})} + \mathbf{g} * (I + \overline{S}') \cdot \mathbf{R} = 0 \tag{4.9}$$

where $(\cdot)$ is the regular one index inner product.

### 4.2. Calculation of $\langle R \rangle$

Similar to the single constraint case, our first interest is to find "how far" is $\langle \mathbf{R} \rangle$ from $\mathbf{R}^{(\mathrm{h})}$. Define a relative difference matrix $\mathbf{D}$ by:

$$\mathbf{R} = (\mathbf{I} + \mathbf{D}) \cdot \mathbf{R}^{(\mathrm{h})}. \tag{4.10}$$

Substitute Eq. (4.10) in Eq. (4.9), and using Eq. (4.8) we obtain:

$$\left[ (\mathbf{f} + \mathbf{g}) * \overline{S}' + \mathbf{g} * (I + \overline{S}') \cdot \mathbf{D} \right] \cdot \mathbf{R}^{(\mathrm{h})} = 0. \tag{4.11}$$

Since $\mathbf{R}^{(\mathrm{h})}$ does not contain statistical information, the expression in brackets must vanish. Therefore,

$$\mathbf{D} = -(\mathbf{g} * (I + \overline{S}'))^{-1} \cdot \mathbf{h} * \overline{S}'; \quad \mathbf{h} = \mathbf{f} + \mathbf{g}. \tag{4.12a, b}$$

Expansion any function $\mathbf{D}(\overline{S}')$ around $S' = 0$ and averaging yields

$$\langle \mathbf{D} \rangle = \tfrac{1}{2} \mathbf{D}_{,\overline{S}'\overline{S}'} \Big|_0 * * \langle \overline{S}' \overline{S}' \rangle + \mathrm{o}(\overline{S}'^3). \tag{4.13}$$

Differentiation, using Eqs. (4.8) and (4.12) and the symmetry of $\mathbf{G}$ we obtain:

$$\mathbf{D}_{,\overline{S}'} = (\mathbf{g} * (I + \overline{S}'))^{-1} \cdot \mathbf{g} \cdot \mathbf{h}^{\mathrm{T}} \cdot (\mathbf{g} * (I + \overline{S}'))^{-1} - (\mathbf{g} * (I + \overline{S}'))^{-1} \cdot \mathbf{h}, \tag{4.14}$$

$$\tfrac{1}{2} \mathbf{D}^{(0)}_{,\overline{S}'\overline{S}'} = \tfrac{1}{2} \mathbf{D}_{,\overline{S}'\overline{S}'} \Big|_0 = \mathbf{G}^{-1} \cdot \mathbf{g} \cdot \mathbf{h}^{\mathrm{T}} \cdot \mathbf{G}^{-1}. \tag{4.15}$$

Therefore

$$\langle \mathbf{D} \rangle \cong \mathbf{G}^{-1} \cdot (\mathbf{g}_{\cdot}^{*\langle \overline{S}' \overline{S}' \rangle *} \mathbf{h}^{\mathrm{T}}) \cdot \mathbf{G}^{-1}, \tag{4.16}$$

where the product between $\mathbf{g}$ and $\mathbf{h}^{\mathrm{T}}$ in Eq. (4.16) contains both inner product and integration.

### 4.3. Variance of R and the generalized reciprocal relation

By definition

$$\mathbf{V}(\mathbf{R}) = \langle \mathbf{R}\mathbf{R} \rangle - \langle \mathbf{R} \rangle \langle \mathbf{R} \rangle = \langle (\Delta \mathbf{R})(\Delta \mathbf{R}) \rangle; \quad \Delta \mathbf{R} = \mathbf{R} - \langle \mathbf{R} \rangle, \tag{4.17}$$

where $\mathbf{V}$ is a second order tensor. Expansion of $\mathbf{R}(\mathbf{S})$ around $\langle S \rangle$, inserting in Eq. (4.17), the first order approximation is:

$$\mathbf{V}(\mathbf{R}) \cong \mathbf{R}_{,S'} \big|_0 * \langle S' S' \rangle * \mathbf{R}_{,S'} \big|_0. \tag{4.18}$$

Note that Eq. (4.17) involves both integration and outer vector product (diad). Now, using Eq. (4.9), differentiation and inserting in Eq. (4.17) yields

$$\mathbf{V}(\mathbf{R}) \cong \mathbf{R}^{(\mathrm{h})} \cdot \left[\mathbf{D}_{,S'} * \langle S'S' \rangle * \mathbf{D}^{\mathrm{T}}_{,S'}\right] \cdot \mathbf{R}^{(\mathrm{h})}. \tag{4.19}$$

Inserting Eq. (4.14) in Eq. (4.19) and using Eq. (4.8), an explicit expression for $\mathbf{V}(\mathbf{R})$ is received, which, in component form is

$$V_{mi} = \langle \Delta R_m \Delta R_i \rangle = R^{(\mathrm{h})}_n G^{-1}_{mp} h_{pn} * \langle \overline{S}'\overline{S}' \rangle * h_{kj} G^{-1}_{ik} R^{(\mathrm{h})}_j = V_{im}. \tag{4.20}$$

Taking the dot product on both sides of Eq. (4.20) twice by $G$, we finally get (in component and vector forms):

$$G_{sm} \langle \Delta R_m \Delta R_i \rangle G_{iq} = R^{(\mathrm{h})}_s h_{sn} * \langle \overline{S}'\overline{S}' \rangle * h_{qj} R^{(\mathrm{h})}_q, \tag{4.21a}$$

$$\mathbf{G} \cdot \langle \Delta \mathbf{R} \Delta \mathbf{R} \rangle \cdot \mathbf{G} = \mathbf{R}^{(\mathrm{h})} \cdot \left[\mathbf{h} * \langle \overline{S}'\overline{S}' \rangle * \mathbf{h}^{\mathrm{T}}\right] \cdot \mathbf{R}^{(\mathrm{h})}. \tag{4.21b}$$

Eqs. (4.21a) and (4.21b) provides a *generalized reciprocal relation*: The load variance of the indeterminate, heterogeneous case, operating on the unit displacement matrix of the homogeneous, determinate case, equals the displacement variance of the heterogeneous determinate case, operating on the load vector of the indeterminate homogeneous case.

### 4.4. Displacement average

Inserting Eq. (4.8) in Eq. (4.2) we have

$$w(x) = R^{(\mathrm{h})}_r (h_r + D_{mr} g_m) * (I + \overline{S}'). \tag{4.22}$$

Perturbation around $\langle S \rangle$ and averaging yields

$$\langle w(x) \rangle = w^{(\mathrm{h})}(x) + R^{(\mathrm{h})}_r (\tfrac{1}{2}(g_m * I) D^{(0)}_{mr,\overline{S}'\overline{S}'} * * \langle \overline{S}'\overline{S}' \rangle + D^{(0)}_{mr,\overline{S}'} * \langle \overline{S}'\overline{S}' \rangle * g_m), \tag{4.23}$$

where the derivatives of $D_{mr}$ at $\langle S \rangle$ are given by Eqs. (4.14) and (4.15).

### 4.5. Displacement variance

For weak heterogeneity ($S' \ll \langle S \rangle$), the first-order approximation for $V(w(x))$ is Eq. (A.35).

$$V(w(x;\overline{S}')) = w^{(0)}_{,\overline{S}'} * \langle \overline{S}'\overline{S}' \rangle * w^{(0)}_{,\overline{S}'}. \tag{4.24}$$

Using Eqs. (4.8), (4.12) and (4.22), and after some algebra,

$$V(w(x;\overline{S}')) = [g_m * II * g_n] \left\{ G^{-1}_{mp} h_{pr} R^{(\mathrm{h})}_r * \langle \overline{S}'\overline{S}' \rangle * R^{(\mathrm{h})}_s h_{qs} G^{-1}_{nq} \right\}, \tag{4.25}$$

or, in a more symmetric form:

$$V(w(x;\overline{S}')) = \boldsymbol{\gamma} \cdot \mathbf{G}^{-1} \cdot \mathbf{H} \cdot \mathbf{G}^{-1} \cdot \boldsymbol{\gamma}, \tag{4.26}$$

where

$$\gamma_m = g_m * I; \quad H_{pq} = R^{(\mathrm{h})}_r h^{\mathrm{T}}_{rp} * \langle \overline{S}'\overline{S}' \rangle * h_{qs} R^{(\mathrm{h})}_s. \tag{4.27}$$

Note that $\mathbf{H}$ is the displacement variance for a determinate heterogeneous beam, loaded by the "homogeneous forces", $\mathbf{G}$ is the displacement matrix of a homogeneous determinate beam and $\gamma$ is the displacement at $x$. Therefore, right-hand side of Eq. (4.26) is found from different solutions of determinate

problems. Another important observation from Eq. (4.25) is that since $V = 0$ both for correlation range of 0 and $L$, there must be a specific range for which maximal displacement variance is obtained.

## 5. Conclusions

(1) Average values and associated statistical variances can be obtained analytically for weak heterogeneity by first-order perturbation.

(2) Average response such as deflections and reaction forces of statically indeterminate micro-beams, are functions of the structure and the type of loading. Therefore, their values cannot be calculated directly by using the effective moduli, based on RVE. Specific bounds for the differences between micro- and macro-beams, and the corresponding load distributions can be found analytically for simple cases.

(3) The above differences, as well as statistical variances, are sensitive to the compliance statistical correlation range. However, there is always a specific range for which these parameters are maximal.

(4) For weak heterogeneity, statistical parameters of indeterminate cases can be obtained by superposition of corresponding solutions (both averages and variances) of determinate problems.

## Acknowledgements

Partial support of the Technion IIT fund for research advancement and the support of the Weizmann Institute of Science, Rehovot, Israel, is gratefully acknowledged. The author wishes to thank Dr. M. Zeifman from the Technion for his valuable assistance during the initial stage of this study.

## Appendix A. Mathematical definitions and notations

The purpose of the appendix is to lay out different algebraic manipulations needed for the analysis in the text.

### *A.1. Products and integration of scalar functions and functionals*

Given two functions $f^{\mathrm{I}}(x_1)$, and $g^{\mathrm{I}}(x_2)$, of one variable each, three types of products are useful: dyadic product,

$$f^{\mathrm{I}}g^{\mathrm{I}} \equiv f^{\mathrm{I}}(x_1)g^{\mathrm{I}}(x_2) = h^{\mathrm{II}}(x_1, x_2). \tag{A.1}$$

Inner product:

$$f^{\mathrm{I}} \circ g^{\mathrm{I}} \equiv f^{\mathrm{I}}(x_1)g^{\mathrm{I}}(x_1) \tag{A.2}$$

and inner integral product (convolution):

$$f^{\mathrm{I}} * g^{\mathrm{I}} \equiv f^{\mathrm{I}}(x_1) * g^{\mathrm{I}}(x_2) = \int f^{\mathrm{I}}(x) * g^{\mathrm{I}}(x)\,\mathrm{d}x. \tag{A.3}$$

For functions of two variables ($f^{\mathrm{II}}$, $g^{\mathrm{II}}$), a generalized definition is:

$$f^{\mathrm{II}}g^{\mathrm{II}} \equiv f^{\mathrm{II}}(x_1, x_2)g^{\mathrm{II}}(x_3, x_4), \qquad f^{\mathrm{II}} \circ g^{\mathrm{II}} \equiv f^{\mathrm{II}}(x_1, x_2)g^{\mathrm{II}}(x_2, x_3), \tag{A.4}$$

and

$$f^{\mathrm{II}} * g^{\mathrm{II}} \equiv \int f^{\mathrm{II}}(x_1, x) * g^{\mathrm{II}}(x, x_2)\,\mathrm{d}x. \tag{A.5}$$

A "mixed" form is defined similarly

$$f^{\mathrm{II}} * g^{\mathrm{I}} \equiv \int f^{\mathrm{II}}(x_1, x) * g^{\mathrm{I}}(x)\,\mathrm{d}x. \tag{A.6}$$

Products of functions of more than two variables will not be used here, so the notations ($^{\mathrm{I}}$), ($^{\mathrm{II}}$) can be omitted without causing confusion. Define a transpose function by

$$f(x_1, x_2) = f(x_2, x_1)^{\mathrm{T}}, \tag{A.7}$$

$$f * g^{\mathrm{T}} \equiv \int f(x_1, x) * g(x_2, x)\,\mathrm{d}x. \tag{A.8}$$

The above is equivalent to inner product operations of tensors. For example,

$$(f * g)^{\mathrm{T}} \equiv g^{\mathrm{T}} * f^{\mathrm{T}}. \tag{A.9}$$

If $s$ is a two-variable "functionally" symmetric function, we have

$$s(x_1, x_2) = s(x_2, x_1) \iff s^{\mathrm{T}} = s. \tag{A.10}$$

Combining Eqs. (A.6)–(A.8), the following double integration form, involving a symmetric function ($s$), appears frequently in the analysis

$$f * s * g^{\mathrm{T}} = g * s * f^{\mathrm{T}}. \tag{A.11}$$

Furthermore,

$$(f + g) * s * (f + g)^{\mathrm{T}} \equiv f * s * f^{\mathrm{T}} + 2g * s * f^{\mathrm{T}} + g * s * g^{\mathrm{T}}, \tag{A.12}$$

which means that any expression like Eq. (A.9) can be written as a sum of "symmetric" forms.

Two types of "unit" operations are used. The first is a one variable function $I(x) = 1$, for which

$$f^{\mathrm{I}} * I \equiv \int f^{\mathrm{I}}(x)\,\mathrm{d}x; \quad f^{\mathrm{I}} \circ I = f^{\mathrm{I}} \tag{A.13}$$

and similarly

$$f^{\mathrm{II}} * I = \int f^{\mathrm{II}}(x_1, x_2) I(x_2)\,\mathrm{d}x_2 = \int f^{\mathrm{II}}(x_1, x_2)\,\mathrm{d}x_2, \tag{A.14}$$

By the same notation, "double integration" is used too:

$$f * * g^{\mathrm{T}} = \int\int f(x_1, x_2) g(x_2, x_1)\,\mathrm{d}x_1\,\mathrm{d}x_2 \tag{A.15}$$

$$f^{\mathrm{II}} * * II = f^{\mathrm{II}} * I * I = \int f^{\mathrm{II}}(x_1, x_2)\,\mathrm{d}x_1\,\mathrm{d}x_2, \tag{A.16}$$

where $II$ is the unit dyad. Thus,

$$I * I = x, \tag{A.17}$$

$$f * II * g = \int\int f(x_1 x_2) I(x_2) I(x_2) g(x_3, x_4)\,\mathrm{d}x_2\,\mathrm{d}x_3 \tag{A.18}$$

$$= \int\int f(x_1, x_2) g(x_3, x_4)\mathrm{d}x_2\,\mathrm{d}x_3 = (f * I)(g^{\mathrm{T}} * I). \tag{A.19}$$

The second unit operator is a two variable Dirac function $\delta(x_1,x_2)$, for which

$$f*\delta=\int f(x_1,x_2)\delta(x_2,x_3)\,\mathrm{d}x_2=f(x_1,x_3)=f \tag{A.20}$$

and therefore

$$f*\delta*g^{\mathrm{T}}=f*g^{\mathrm{T}}. \tag{A.21}$$

We see that $(\delta)$ "eliminates" integrations, and $(I)$ "separates" them. When specific limits of integration are involved, a convenient notation is

$$f\underset{a}{\overset{b}{*}}g\equiv\int_a^b f(x_1,x_2)g(x_2,x_3)\,\mathrm{d}x_2. \tag{A.22}$$

For example,

$$\int_{b_1}^{b_2}\mathrm{d}x_3\int_{a_1}^{a_2}f(x_1,x_2)s(x_2,x_3)g(x_4,x_3)\,\mathrm{d}x_2\equiv f\underset{a_1}{\overset{a_2}{*}}s\underset{b_1}{\overset{b_2}{*}}g^{\mathrm{T}}. \tag{A.23}$$

Differentiation by the limit points yield the inverse integral operation:

$$\frac{\partial}{\partial b}f\underset{a}{\overset{b}{*}}g=f\circ g;\qquad\frac{\partial}{\partial a}f\underset{a}{\overset{b}{*}}g=-f\circ g. \tag{A.24}$$

A special case of a double integration as in (A.11) is the case where $s(x_2,x_3)$ is non-zero in a small region $(\lambda)$ near $x_2=x_3$.

$$f*s*g^{\mathrm{T}}=\sigma\lambda(f*\delta*g^{\mathrm{T}})=\sigma(f*g^{\mathrm{T}});\quad\sigma=\lambda(s*I), \tag{A.25}$$

where $\sigma$ is some average value in $\lambda$. Furthermore, for this special case,

$$f\underset{a_1}{\overset{a_2}{*}}s\underset{b_1}{\overset{b_2}{*}}g^{\mathrm{T}}=f\underset{c_1}{\overset{c_2}{*}}s\underset{c_1}{\overset{c_2}{*}}g^{\mathrm{T}};\qquad[c_1,c_2]=[a_1,a_2]\cap[b_1,b_2]. \tag{A.26}$$

Also, for convenience

$$f\underset{a_1}{\overset{a_2}{*}}s+g^{\mathrm{T}}\underset{b_1}{\overset{b_2}{*}}s\equiv(f\underset{a_1}{\overset{a_2}{*}})+g^{\mathrm{T}}\underset{b_1}{\overset{b_2}{*}}))s,\ \text{etc.} \tag{A.27}$$

A special unit operation involving variation is

$$\frac{\delta(f*g)}{\delta f}=\delta*g=g, \tag{A.28}$$

where $\delta$ is used both for variation and for Dirac operator.

### *A.2. Statistical relations of functionals*

Consider a functional $R(S)$ of a random function $S(x)$. Two types of averages are defined in text. The regular $\langle R\rangle$ and the "homogeneous" one

$$R_{\mathrm{h}}=R(\langle S\rangle) \tag{A.29}$$

with associated variances

$$V(R) = \langle (R - \langle R \rangle)^2 \rangle \quad \text{and} \quad V_{\mathrm{h}}(R) = \langle (R - R_{\mathrm{h}})^2 \rangle. \tag{A.30}$$

By definition, the averages and variances are related by:

$$V_{\mathrm{h}} - V = (R_{\mathrm{h}} - \langle R \rangle)^2. \tag{A.31}$$

For small variations of $S$ around its average,

$$R(S) = R\Big|_{S=\langle S \rangle} + R_{,S}\big|_{\langle S \rangle} * \delta S + \tfrac{1}{2} R_{,SS}\big|_{\langle S \rangle} * * \delta S^2 + \cdots \tag{A.32}$$

where

$$R_{,S}\big|_{\langle S \rangle} * \delta S = \frac{\delta R}{\delta S}\bigg|_{\langle S \rangle} * \delta S \equiv \int \frac{\delta R}{\delta S(x)}\bigg|_{\langle S \rangle} \delta S(x)\, \mathrm{d}x; \tag{A.33}$$

$$R_{,SS}\big|_{\langle S \rangle} * * \delta S^2 = \frac{\delta^2 R}{\delta S^2}\bigg|_{\langle S \rangle} * * \delta S^2 \equiv \int \int \frac{\delta}{\delta S(x_2)} \left(\frac{\delta R}{\delta S(x_1)}\right)\bigg|_{\langle S \rangle} \delta S(x_1) \delta S(x_2)\, \mathrm{d}x_1\, \mathrm{d}x_2. \tag{A.34}$$

Using the above, the first order approximation of $V$ is:

$$V(R) \cong (R_{,S})^2\Big|_{\langle S \rangle}, \tag{A.35}$$

which holds for any tensor function of $S$.

### A.3. Mixed operations with tensors

Consider a function $S(x)$, a vector functional ($\mathbf{R}(S(x))$) and two second-order tensor functions ($\mathbf{g}(x)$, $\mathbf{h}(x)$). Outer (diadic) product is written without any additional symbol

$$\begin{aligned} &\mathbf{RR} \text{ – second-order tensor functional with components : } R_i(S(x_1))R_j(S(x_2)),\\ &\mathbf{gh} \text{ – fourth-order tensor function of two variables with components : } g_{ij}(x_1)h_{kl}(x_2). \end{aligned} \tag{A.36}$$

Similarly, tensor inner products are written as

$$\begin{aligned} &\mathbf{g} \cdot \mathbf{h} \text{ – second-order tensor function with components : } g_{ij}(x_1)h_{jk}(x_2),\\ &\mathbf{g} \cdot \cdot \mathbf{h}^{\mathrm{T}} - \text{ scalar function with components : } g_{ij}(x_1)h_{ij}(x_2). \end{aligned} \tag{A.37}$$

Convolution product operation is identical with the scalar functional case

$$\begin{aligned} &\mathbf{g} * S \text{ – second-order tensor : } \int g_{ij}(x_1)S(x_1)\, \mathrm{d}x_1,\\ &\mathbf{g} * \langle SS \rangle * \mathbf{h} \text{ – fourth-order tensor : } \int g_{ij}(x_1)\langle S(x_1)S(x_2)\rangle h_{kl}(x_2)\, \mathrm{d}x_1\, \mathrm{d}x_2. \end{aligned} \tag{A.38}$$

The variation of $\mathbf{R}$ with respect to $S$ is

$$\delta \mathbf{R} = \mathbf{R}_{,S} * \delta S \text{ where } \mathbf{R}_{,S} \text{ is a vector functional of } S \text{ and a vector function of } x. \tag{A.39}$$

Finally, a mixed operation is also used in the text

$\mathbf{g} \overset{*\langle SS \rangle *}{\cdot} \mathbf{h}$ – second-order tensor with components

$$\int \int g_{ij}(x_1)\langle S(x_1)S(x_2)\rangle h_{jk}(x_2)\, \mathrm{d}x_1\, \mathrm{d}x_2. \tag{A.40}$$

## References

Beran, M.J., Mason, T.A., Adams, B.L., Olsen, T., 1996. Bounding elastic constants of an orthotropic polycrystal using measurement of micro-structure. J. Mech. Phys. Solids 44, 1543–1563.

Beran, M.J., 1998. The use of classical beam theory for micro-beams composed of polycrystals. Int. J. Solids Struct. 35 (19), 2407–2412.

Box, G., Jenkins, G., 1970. Time Series Analysis Forcasting and Control. Holden-Day, San Francisco, CA.

Drugan, W.J., Willis, J.R., 1996. A micro-mechanics-based non-local constitutive equation and estimates of representative volume element size for elastic composites. J. Mech. Phys. Solids 44 (4), 497–524.

Hashin, Z., Shtrikman, S., 1962. A variational approach to the theory of the elastic behavior of polycrystals. J. Mech. Phys. Solids 10, 343–352.

Howe, T.R., Muller, R.S., 1983. Polycrystalline silicon micro-mechanical beams. J. Electrochem. Soc. 130 (6), 1420–1423.

Howe, T.R., 1988. Applications of polysilicon films in micro-sensors and micro-actuators. Mat. Res. Symp. Proc., Materials Research Society, 106, 213–223.

Jones, P.T., Johnson, G.C., Howe, R.T., 1998. Fracture strength of polycrystalline silicon. Maer. Res. Soc. Symp. Proc. 518, 197–203.

Kamins, T., 1998. Polycrystalline Silicon for Integrated Circuits and Displays. Kluwer Academic Press, Dordrecht.

Kroner, E., 1986. Statistical Modelling. In: Gittus, J., Zarka, J. (Eds.), Modeling Small Deformation of Polycrystals, Elsevier, Amsterdam, pp. 229–291 (Chapter 8).

Madou, M., 1997. Fundamentals of Micro-fabrication. CRC Press, Boca Raton, FL, p. 217.

Mason, T.A., Adams, B.L., 1999. Use of micro-structural statistics in predicting polycrystalline material properties. Metall. Mat. Trans. A 30, 969–979.

Mirfendereski, D., Kiureghian, A., Ferrari, M., 1992. Analysis of micro-fabricated textured multicrystalline beams: II. Probabilistic approach. Mater. Res. Symp. Proc., Materials Research Society 276, 97–101.

Ostoja-Starzewski, M., 1998. Random field models of heterogeneous materials. Int. J. Solids Struct. 35 (19), 2429–2455.

Serre, C., Gorostiza, P., Perez-Rodriguez, A., Sanz, F., Morante, J.R., 1998. Determination of micro-mechanical properties of polysilicon micro-structures with an atomic force microscope. Sensors Actuators A 67, 215–219.

Serre, C., Perez-Rodriguez, A., Morante, J.R., Gorostiza, P., Esteve, J., 1999. Determination of micro-mechanical properties of thin films by beam bending measurements with an atomic force microscope. Sensors Actuators A 74, 134–138.

Somoroff, A., 1970. A variational approach to statistically non-homogeneous fields. Quart. Appl. Math. 28 (2), 219–236.

Willis, J.R., 1977. Bounds and self consistent estimates for the overall properties of anisotropic composites. J. Mech. Phys. Solids 25, 185–202.

Wortman, J.J., Evans, R.A., 1965. Young's modulus, Shear modulus and Poisson's ratio in silicon and germanium. J. Appl. Phys. 36 (1), 153–156.